Electrical Power and Energy Systems 31 (2009) 302–308

Contents lists available at ScienceDirect

Electrical Power and Energy Systems

journal homepage: www.elsevier.com/locate/ijepes

A Lyapunov theory based UPFC controller for power flow control

Ali Zangeneh *, Ahad Kazemi, Majid Hajatipour, Shahram Jadid

Center of Excellence for Power Systems Automation and Operation, Iran University of Science and Technology, Tehran, Iran

ARTICLE INFO

Article history:
Received 20 February 2007
Received in revised form 22 February 2009
Accepted 16 March 2009

Keywords:
FACTS
Lyapunov theory
Power flow control
UPFC

ABSTRACT

Unified power flow controller (UPFC) is the most comprehensive multivariable device among the FACTS controllers. Capability of power flow control is the most important responsibility of UPFC. According to high importance of power flow control in transmission lines, the proper controller should be robust against uncertainty and disturbance and also have suitable settling time. For this purpose, a new controller is designed based on the Lyapunov theory and its stability is also evaluated. The Main goal of this paper is to design a controller which enables a power system to track reference signals precisely and to be robust in the presence of uncertainty of system parameters and disturbances. The performance of the proposed controller is simulated on a two bus test system and compared with a conventional PI controller. The simulation results show the power and accuracy of the proposed controller.

1. Introduction

Nowadays the grow of power systems will rely more on increasing capability of existing transmission systems, rather than on building new transmission lines and power stations, for economical and environmental reasons. Due to deregulation electricity markets, the need for new power flow controllers capable of increasing transmission capability, controlling power flows through predefined corridors and ensuring the security of energy transactions will certainly increase.

The potential benefits with the utilization of flexible ac transmission system (FACTS) devices include reduction of operation and transmission investment costs, increasing system security and reliability, and increasing transfer capabilities in a deregulated environment. FACTS devices are able to change, in a fast and effective way, the network parameters to achieve a better system performance [1].

Unified Power Flow Controller (UPFC) is the most comprehensive multivariable device among the FACTS controllers [2]. Simultaneous control of multiple power system variables with UPFC imposes enormous difficulties. In addition, the complexity of the UPFC control increases due to the fact that the controlled and the control variables interact with each other.

UPFC is a power electronic based device which can provide a proper control for impedance, phase angle and reactive power of a transmission line [2]. Each converter of a UPFC can independently generate or absorb reactive power. This arrangement enables free flow of active power in either direction between the ac terminals of the two converters [3]. In the case of the parallel branch of UPFC, the active power exchanged with the system, primarily depends on the phase shift of the converter output voltage with respect to the system voltage, and the reactive power is controlled by varying the amplitude of the converter output voltage. However series branch of UPFC controls active and reactive power flows in the transmission line by amplitude and phase angle of series injected voltage. Therefore active power controller can significantly affect the level of reactive power flow and vice versa.

In recent years a number of investigations have been carried out on various capabilities of UPFC such as power flow control [3–8], voltage control [9,10], transient stability enhancement [11,12], oscillation damping [13–16]. It has been reported in the literatures that there exists a strong dynamic interaction between active and reactive power flows through a transmission line when they are controlled by series injected voltage v_{se} of the UPFC. Zou et al. [17] presented a non-linear index based on normal forms theory to investigate interaction among UPFC controllers (power flow controller, AC voltage controller and DC voltage controller). A P-Q decoupled control scheme based on fuzzy neural network proposed in [18] to improve dynamic control performance. Their proposed controller reduced the inevitable interactions between real and reactive power flow control. It is very difficult to independently control the active/reactive power flow through the line without affecting the reactive/active power flow. Nevertheless, independent control of active and reactive power flows is sometimes necessary to improve the performance of the UPFC. For this reason, a decoupled control strategy based on d–q axis theory is first proposed in [19].

The performance of the control scheme deteriorates in the presence of uncertainties in system parameters. In this paper, a new controller of UPFC based on Lyapunov theory for power flow control is designed which is able to track reference signals precisely

* Corresponding author. Tel.: +98 21 73912964; fax: +98 21 77491242.
E-mail address: zangeneh@iust.ac.ir (A. Zangeneh).

0142-0615/$ - see front matter © 2009 Elsevier Ltd. All rights reserved.
doi:10.1016/j.ijepes.2009.03.005

and is robust in the presence of uncertainty of system parameters and disturbances The proposed controller is considered as slope changes of energy function which always consists of a set of error terms to provide stability condition in the presence of uncertainty and disturbance.

The remaining section of this paper is set off as follows: Section 2 describes shunt and series branches model of UPFC in the state space. In Section 3, Lyapunov theory based controller is illustrated and simulation results in a typical two bus system are presented in Section 4. Finally Section 5 provides some concluding results.

2. UPFC model

The schematic diagram of a UPFC is shown in Fig. 1. It consists of two back-to-back, self-commutated, voltage source converters connected through a common dc link [8].

As it can be seen in Fig. 1, converter1 is coupled to the AC system through a shunt transformer (excitation transformer) and the converter 2 is coupled through a series transformer (boosting transformer). Note that, subscripts '*s*' and '*r*' are used to represent sending and receiving end buses respectively. By regulating the series injected voltage v_{se}, the complex power flow $(P_r + jQ_r)$ through the transmission line can be controlled. The complex power injected by the converter 2, $(P_{se} + jQ_{se})$ depends on its output voltage and transmission line current. The injected active power P_{se} of the series converter is taken from the dc link, which is in turn drawn from the AC system through the converter 1. On the other hand, both converters are capable of absorbing or supplying reactive power independently. The reactive power of the converter 1 can be used to regulate the voltage magnitude of the bus at which the shunt transformer is connected.

The single-phase representation of a three-phase UPFC system is shown in Fig. 2. In this figure both converters are represented by voltage sources v_{se} and v_{sh}, respectively. Also $(R = R_{se} + R_L)$ and $(L = L_{se} + L_L)$ represent the resistance and leakage inductance of series transformer and transmission line respectively, similarly R_{sh} and L_{sh} represent the resistance and leakage inductance of the shunt transformer respectively [8].

The current through the series and shunt branches of the circuit of Fig. 2 can be expressed by the following differential equations for one phase of the system [8]. These equations can be written for other phases similarly.

$$\frac{di_{sea}}{dt} = \frac{1}{L}(-Ri_{sea} + v_{sea} + v_{sa} - v_{ra}) \tag{1}$$

$$\frac{di_{sha}}{dt} = \frac{1}{L}(-Ri_{sha} + v_{sha} - v_{sa}) \tag{2}$$

The three-phase system differential equations can be transformed into a "*d*, *q*" reference frame using Park's transformation as follows:

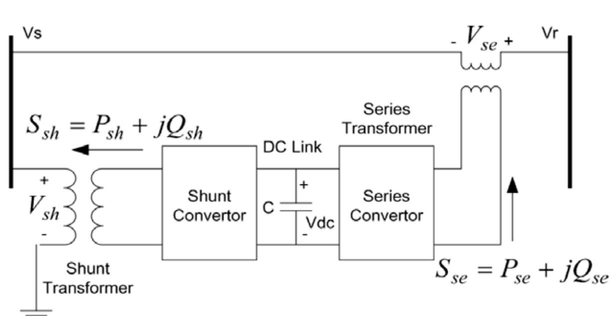

Fig. 1. Schematic diagram of the UPFC system.

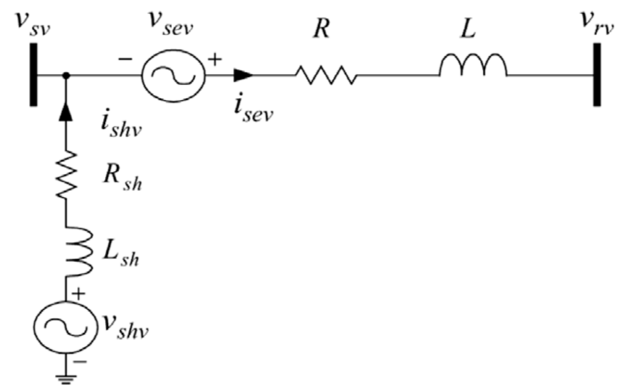

Fig. 2. Single phase representation of the UPFC system.

$$\begin{bmatrix} \dot{i}_{sed} \\ \dot{i}_{seq} \end{bmatrix} = \begin{bmatrix} \frac{-R}{L} & \omega_b \\ -\omega_b & \frac{-R}{L} \end{bmatrix} \cdot \begin{bmatrix} i_{sed} \\ i_{seq} \end{bmatrix} + \frac{1}{L} \begin{bmatrix} v_{sed} + v_{sd} - v_{rd} \\ v_{seq} - v_{rq} \end{bmatrix} \tag{3}$$

$$\begin{bmatrix} \dot{i}_{shd} \\ \dot{i}_{shq} \end{bmatrix} = \begin{bmatrix} \frac{-R_{sh}}{L_{sh}} & -\omega_b \\ -\omega_b & \frac{-R_{sh}}{L_{sh}} \end{bmatrix} \cdot \begin{bmatrix} i_{shd} \\ i_{shq} \end{bmatrix} + \frac{1}{L_{sh}} \begin{bmatrix} v_{shd} + v_{sd} \\ v_{shq} \end{bmatrix} \tag{4}$$

where $\omega_b = 2\pi f_b$, and f_b is the fundamental frequency of the supply voltage. Since the Park's transformation used in finding (3) and (4) keeps the instantaneous power invariant and the *d*-axis lies on the space vector of the sending end voltage v_s, thus $v_s = (v_{sd} + jv_{sq}) = (v_{sd} + j0)$.

Note that in the above equations, subscripts '*d*' and '*q*' are used to represent the direct and quadrature axes components, respectively $(x = x_d + jx_q)$.

Since the dynamic equations of converter 1 are identical to that of converter 2 as described before, both converters should have identical control strategy. Therefore for the sake of brevity in this paper only the technique of designing the controller of converter 2 is described in detail in the form of state space.

$$\begin{aligned} \dot{\mathbf{x}} &= \mathbf{Ax} + \mathbf{Bu} + d \\ \mathbf{y} &= \mathbf{Cx} \end{aligned} \tag{5}$$

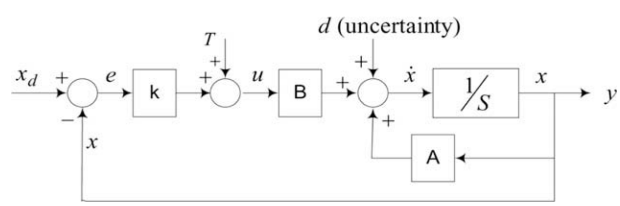

Fig. 3. Schematic of system state space.

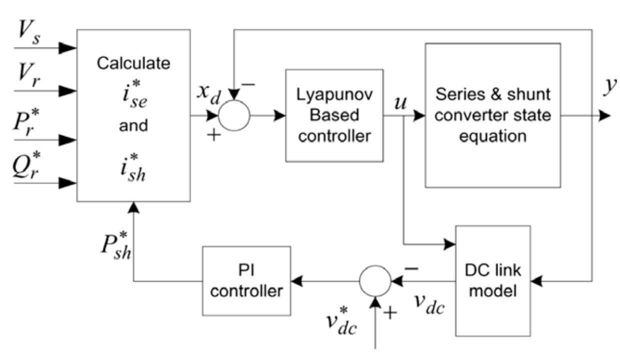

Fig. 4. Block diagram of the overall UPFC control system.

Table 1
Parameters of the PI controllers.

	Converter 1	Converter 2
k_p	0.27	0.3
k_I	61.3	65.6

Table 2
Parameters of the UPFC.

Parameters	$R(pu)$	$\omega L(pu)$	$R_{sh}(pu)$	$\omega L_{sh}(pu)$	$1/\omega C(pu)$
Values	0.05	0.25	0.015	0.15	0.5

where d is the uncertainty vector and $\mathbf{x}$, $\mathbf{u}$ and $\mathbf{y}$ are respectively state, control and output variables vector of converter 2 which are defined as $\mathbf{x} = [i_{sed} \quad i_{seq}]^T$, $\mathbf{u} = [v_{sed} \quad v_{seq}]^T$ and $\mathbf{y} = [i_{sed} \quad i_{seq}]^T$. Comparing Eqs. (3) and (5), when v_s and v_r are kept constant, the system matrices $\mathbf{A}$, $\mathbf{B}$, and $\mathbf{C}$ can be written as:

$$\mathbf{A} = \begin{bmatrix} -R/L & \omega_b \\ -\omega_b & -R/L \end{bmatrix}; \quad \mathbf{B} = \begin{bmatrix} 1/L & 0 \\ 0 & 1/L \end{bmatrix}; \quad \mathbf{C} = \begin{bmatrix} 1 & 0 \\ 0 & 1 \end{bmatrix} \tag{6}$$

As mentioned previously, the common connection between the two converters is formed by a dc-voltage bus. When the losses in the converters are neglected, the active power balance equation at the dc link can be written as [8]:

$$P_{dc} = P_{se} + P_{sh} \tag{7}$$

where P_{sh} and P_{se} are active power supplied by the converters 1 and 2, respectively which can be obtained as follows:

$$P_{se} = \frac{3}{2}(v_{sed}i_{sed} + v_{seq}i_{seq}) \tag{8}$$

$$P_{sh} = \frac{3}{2}(v_{shd}i_{shd} + v_{shq}i_{shq}) \tag{9}$$

Note that, since the power loss of the shunt transformer can be ignored, active power of converter 1 (9) can be written approximately as:

$$P_{sh} \approx \frac{3}{2}(v_{sd}i_{shd}) \tag{10}$$

Also the active power of the dc link is represented as (11):

$$P_{dc} = v_{dc}i_{dc} = -Cv_{dc}\frac{dv_{dc}}{dt} \tag{11}$$

Substituting (11) in (7), (12)will be obtained.

$$\frac{dv_{dc}}{dt} = -\frac{1}{Cv_{dc}}(P_{se} + P_{sh}) \tag{12}$$

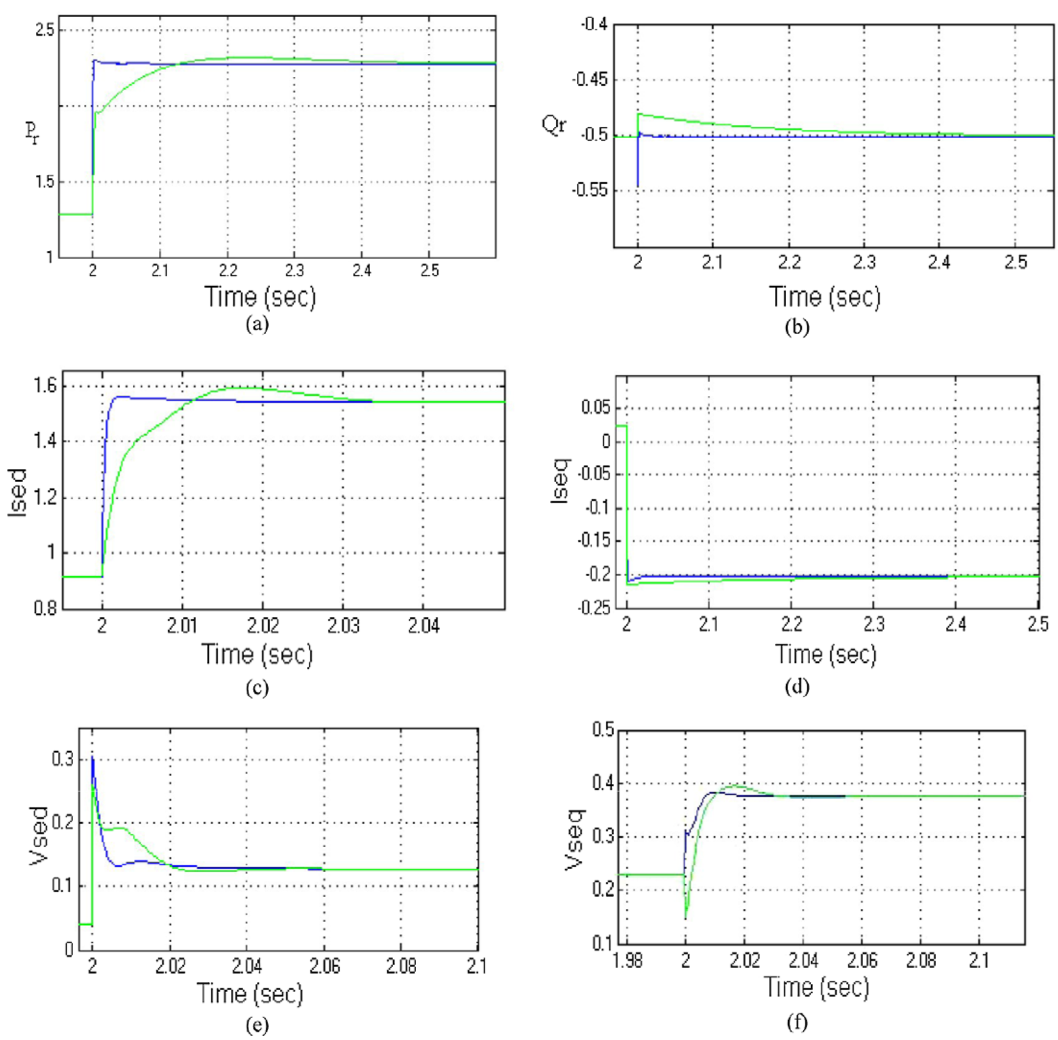

Fig. 5. Response of the UPFC system with 10% uncertainty according to the first case study. Blue line, proposed controller; green line, PID controller. (a) Active power of the transmission line; (b) reactive power of transmission line; (c) direct axis current reference of converter 2; (d) quadrature axis current reference of converter 2; (e) direct axis voltage reference of converter 2; (f) quadrature axis voltage reference of converter 2. (For interpretation of the references to colour in this figure legend, the reader is referred to the web version of this article.)

It is clear that the above equation is non linear, therefore for linearizing and simplifying, Eq. (14) is defined by substituting (13) into (12).

$$\frac{dv_{dc}^2}{dt} = 2v_{dc}\frac{dv_{dc}}{dt} \tag{13}$$

$$\frac{dv_{dc}^2}{dt} = -\frac{2}{C}(P_{se} + P_{sh}) \tag{14}$$

The following section is assigned to introduce the design of a controller based on the Lyapunov theory. This analysis is based on a simplified mathematical model of the converter connected to a two bus system as shown in Fig. 1.

3. Design of a controller based on Lyapunov theory

Fig. 3 shows the schematic of a system state space. As it was mentioned, the main goal of this paper is to design a controller which enables the power system to track reference signals precisely and to be robust in the presence of uncertainty of system parameters and disturbances. To reach this purpose a new controller is designed based on the Lyapunov theory in this paper. The controller based on the Lyapunov method is designed as slope changes of energy function which always remains negative ($\dot{V} < 0$) [20]. This energy function consists of a set of error terms which provides stability condition of error terms in the presence of uncertainty and disturbance. Therefore the tracking error and its derivative are defined as below:

$$\mathbf{e} = \mathbf{x}_d - \mathbf{x} \tag{15}$$

$$\dot{\mathbf{e}} = \dot{\mathbf{x}}_d - \dot{\mathbf{x}} \tag{16}$$

where $\mathbf{x}$ is the vector of state variables and $\mathbf{x}_d = [i_{sed}^* \quad i_{seq}^*]^T$ is the vector of reference signals. In $\mathbf{x}_d$ equation, i_{sed}^* and i_{seq}^* can be obtained similarly by (8) and (9) knowing the active and reactive power references of transmission line ($P_r^*$and Q_r^*)

$$i_{sed}^* = \frac{2}{3}\frac{(P_r^* v_{rd} + Q_r^* v_{rq})}{\Delta} \tag{17}$$

$$i_{seq}^* = \frac{2}{3}\frac{(P_r^* v_{rq} - Q_r^* v_{rd})}{\Delta} \tag{18}$$

where $\Delta = v_{rd}^2 + v_{rq}^2$.

Substituting (15) and (16) in (5), the derivative of tracking (dynamic error) can be obtained:

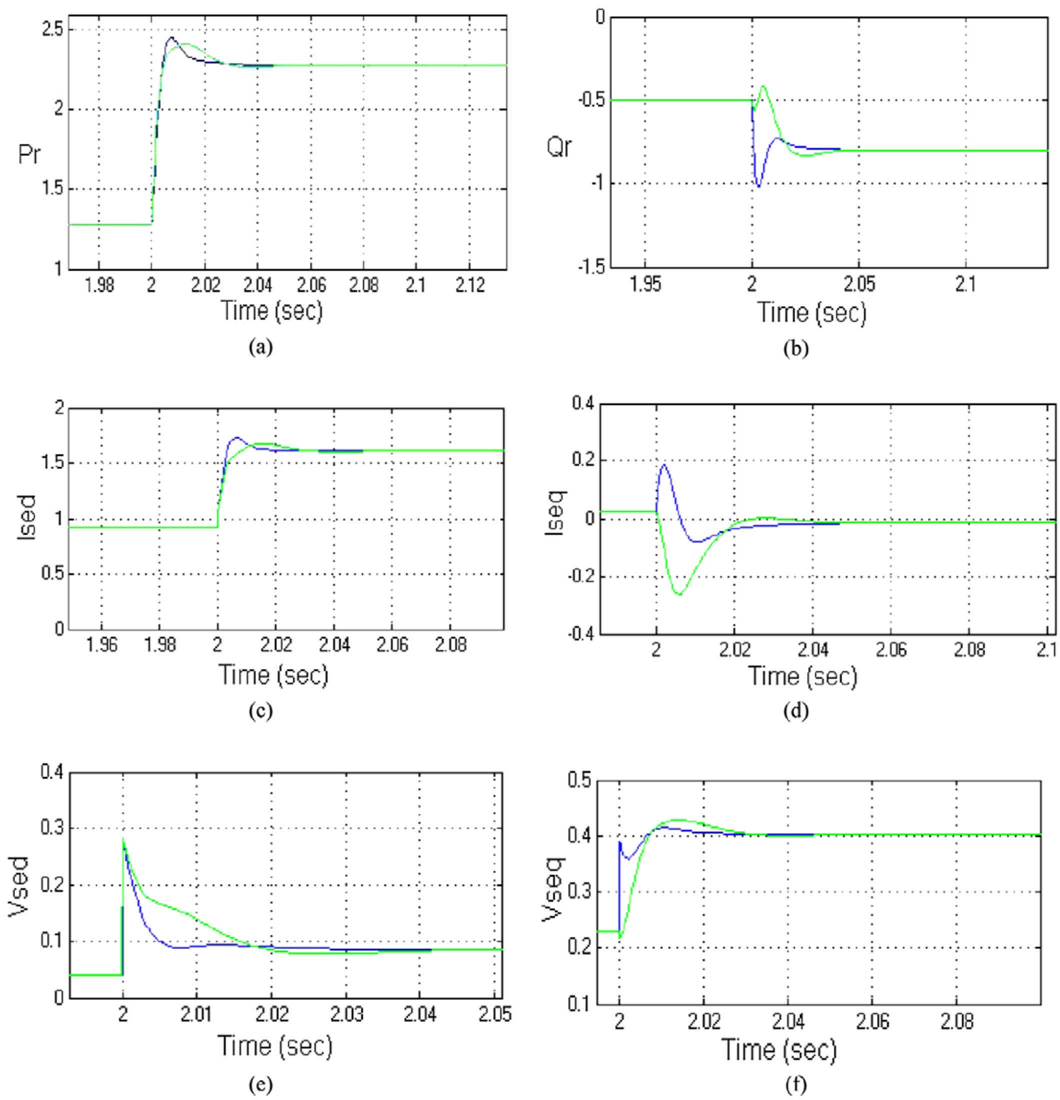

Fig. 6. Response of the UPFC system with 15% uncertainty according to the second case study. Blue line, proposed controller; green line, PID controller. (a) Active power of the transmission line; (b) reactive power of transmission line; (c) direct axis current reference of converter 2; (d) quadrature axis current reference of converter 2; (e) direct axis voltage reference of converter 2; (f) quadrature axis voltage reference of converter 2. (For interpretation of the references to colour in this figure legend, the reader is referred to the web version of this article.)

$$\dot{\mathbf{e}} = \mathbf{Ae} + \dot{\mathbf{x}}_d - \mathbf{Ax}_d - \mathbf{d} - \mathbf{Bu} \tag{19}$$

To fulfill stability condition of the system dynamic error, multiplication of control matrix and control variables vector is defined as:

$$\mathbf{Bu} = \mathbf{Bke} + \dot{\mathbf{x}}_d - \mathbf{Ax}_d - \mathbf{u}_s \tag{20}$$

$$\mathbf{u} = \mathbf{ke} + \mathbf{B}^{-1}(\dot{\mathbf{x}}_d - \mathbf{Ax}_d - \mathbf{u}_s) = \mathbf{ke} + \mathbf{T} \tag{21}$$

The control variables vector (21) is calculated by multiplication of $\mathbf{B}^{-1}$ by (20). The amounts of variables of row matrix $\mathbf{k}$ at (20) are set such as the whole Eigen values of matrix $(\mathbf{A}-\mathbf{Bk})$ are laid on the left side of imaginary axis. Vector $\mathbf{u}_s$ is also values of matrix $(\mathbf{A}-\mathbf{Bk})$ are laid on the left side of imaginary axis. Vector $\mathbf{u}_s$ is also described as a robustness signal. The function of this vector is to accomplish stability condition based on Lyapunov theory. Therefore by substitution equation Eq. (20) into (19), the new equation is obtained for dynamic error of the system [20].

$$\dot{\mathbf{e}} = \mathbf{A}_0\mathbf{e} - \mathbf{d} + \mathbf{u}_s \tag{22}$$

where in the above equation, $\mathbf{A}_0 = \mathbf{A} - \mathbf{Bk}$.

To accomplish stability condition, the robustness signal is defined as below:

$$\mathbf{u}_s = -I^* \frac{|\mathbf{e}^T\mathbf{P}|}{\mathbf{e}^T\mathbf{P}} \cdot d_m = -I^* \cdot d_m \cdot |\mathbf{e}^T\mathbf{P}| \cdot (\mathbf{e}^T\mathbf{P})^{-1} \tag{23}$$

where I^* is a positive number $I^* \geqslant 1$, $\mathbf{P}$ is a positive matrix that is solution of Lyapunov equation (Eq. (II) in Appendix A) and d_{m} is the upper limit of uncertainty which is predicted by designer.

It is necessary to be noted that $(\mathbf{e}^T\mathbf{P})$ is not a square matrix and therefore pseudo inverse matrix is used to calculate $\mathbf{u}_s$ vector [21]. Stability proof of designed controller is presented in Appendix A. The block diagram of the overall UPFC control system is depicted in Fig. 4. This block diagram is implemented for d–q axis.

4. Simulation results

In an ideal system, there is no uncertainty in system parameters. However, in a practical system, it is considered that the

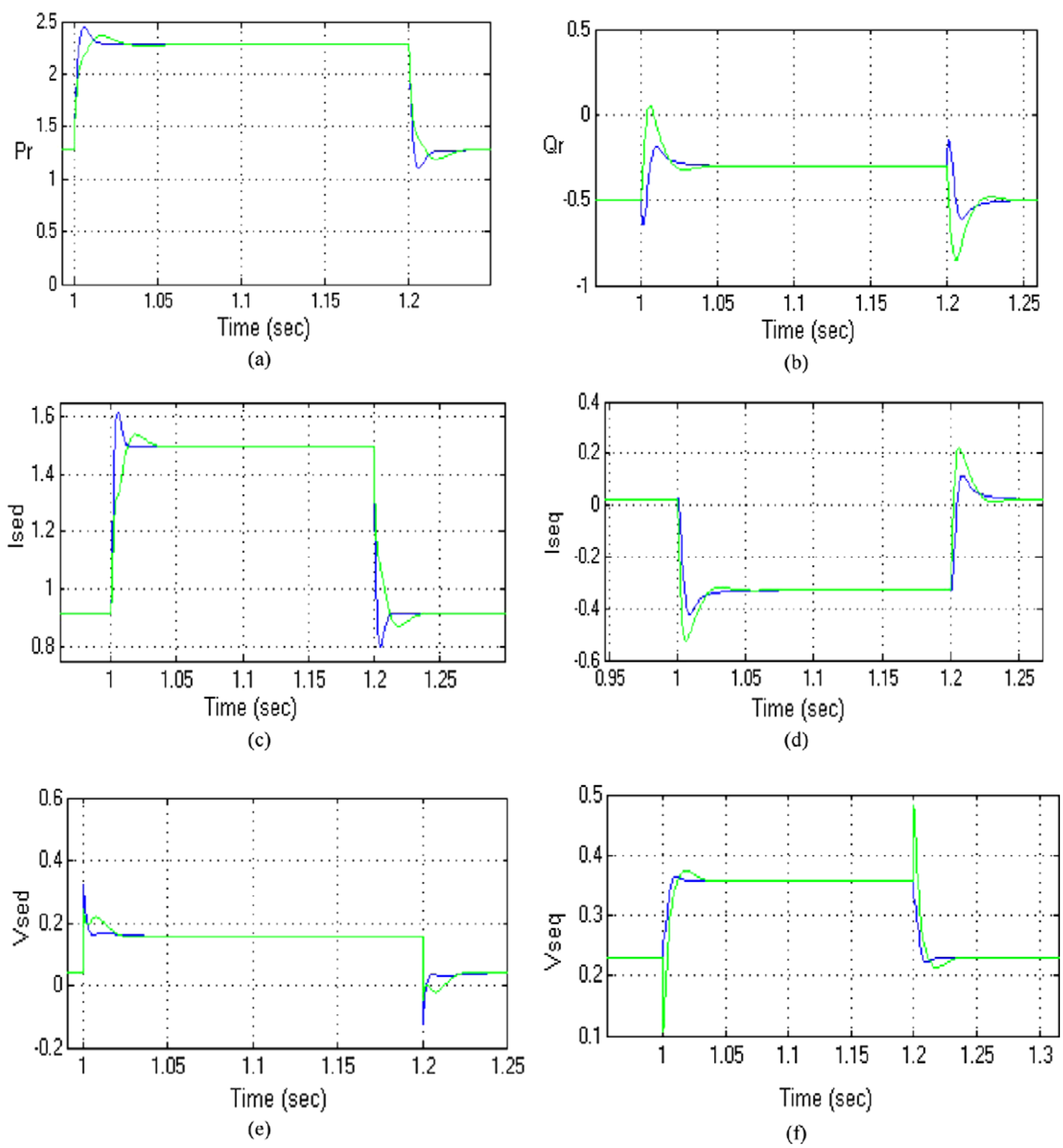

Fig. 7. Response of the UPFC system with 10% uncertainty according to the third case study. Blue line, proposed controller; green line, PID controller. (a) Active power of the transmission line; (b) reactive power of transmission line; (c) direct axis current reference of converter 2; (d): quadrature axis current reference of converter 2; (e) direct axis voltage reference of converter 2; (f) quadrature axis voltage reference of converter 2. (For interpretation of the references to colour in this figure legend, the reader is referred to the web version of this article.)

system parameters are corrupted by some uncertainties. It should be mentioned that such uncertainties are usually present in any physical system and will be often limited to achieve the desired performance [21]. In this paper, the proposed controller is designed so as the uncertainty in the system is reduced. The uncertainty is entered to the system equations as a vector. The performance of the proposed controller, for various disturbances is evaluated through MATLAB/SIMULINK software in a two bus test system. The simulation results of proposed controller are compared with a conventional PI controller. The parameters of converters 1 and 2 of PI controllers are given in Table 1.

According to the parameters of the system and UPFC which are presented in the Table 2, the system matrices for these converters are as follow:

$$A_{se} = 100\pi\begin{bmatrix} -0.2 & 1 \\ -1 & -0.2 \end{bmatrix}, \quad B_{se} = 100\pi\begin{bmatrix} 4 & 0 \\ 0 & 4 \end{bmatrix}$$

$$A_{sh} = 100\pi\begin{bmatrix} -0.1 & 1 \\ 1 & -0.1 \end{bmatrix}, \quad B_{sh} = 100\pi\begin{bmatrix} 6.67 & 0 \\ 0 & 6.67 \end{bmatrix}$$

In the above matrices, fundamental frequency ((f_b) is equal to 50 Hz. In this study, as it is shown in Fig. 4, the sending and receiving end bus voltages are maintained constant and the dc link voltage, active and reactive powers of the transmission line are controlled.

The initial complex power flow ($P_r + jQ_r$) at the receiving end of the transmission line is found as $(1.278 - j0.5)$ pu. In the first case study, the active power of the transmission Line is changed from 1.278 to 2.278 pu at $t = 2$ s for a system with 10% uncertainty. The simulation results of this study are depicted in Fig. 5. It is shown that the speed of response of the proposed controller is much better than that of the conventional controller approach (PI controller).

In the second case study, both the active and reactive powers of the transmission line is changed from initial values to $(2.278 - j0.8)$ at $t = 2$ s. In this case, the uncertainty factor is considered to be equal to 15%. The simulation results of this scenario are displayed in Fig. 6.

As mentioned, the reactive power of the transmission line is changed too and the uncertainty factor is changed much more than previous case, but it is seen that the proposed controller has a good response to this changes.

The active and reactive powers of the transmission line are affected strong disturbance in the latter case study. In this study which is shown in Fig. 7, the active and reactive powers are changed at $t = 1$ s from $(1.278 - j0.5)$ to $(2.278 - j0.3)$ and are changed again to initial value at $t = 1.2$ s. In this case uncertainty factor is considered to be equal to 10%.

Fig. 7 shows the response of the proposed controller for the worst case which is likely occurred. As it can be seen the proposed controller has a powerful approach to trace the system response through the uncertainty and disturbance conditions.

5. Conclusion

The main goal of this paper is to design a controller which enables a power system to track reference signals precisely and to be robust in the presence of uncertainty of system parameters and disturbances. To reach this purpose a new controller is designed based on the Lyapunov theory. The main advantage of the proposed approach with respect to PID controller is the stability of the closed loop system under uncertainties. The proposed approach also has simple structure and quick performance in comparison with intelligence methods such as fuzzy theory and neural network. The intelligence methods usually have long convergence time while they have appropriate performance under uncertainties. The simulation results of the proposed controller are compared with a conventional PI controller and its performance is evaluated in a two bus test system. In this study, the sending and receiving end bus voltages were maintained constant and the dc link voltage, active and reactive powers of the transmission line were controlled. The obtained results from above case studies describe the power, accuracy, fast speed and relatively low overshoot response of the proposed controller.

Appendix A

A.1. Stability proof of designed controller

Consider the following Lyapunov function candidate:

$$V = \frac{1}{2}\mathbf{e}^T\mathbf{P}\mathbf{e} \tag{I}$$

in this equation P is the solution of the Lyapunov equation.

$$\mathbf{A}_0^T\mathbf{P} + \mathbf{P}\mathbf{A}_0 = -\mathbf{Q} \tag{II}$$

where $\mathbf{Q}$ is an arbitrary positive definite matrix. Differentiating V with respect to time gives:

$$\begin{aligned} \dot{V} &= \frac{1}{2}\dot{\mathbf{e}}^T\mathbf{P}\mathbf{e} + \frac{1}{2}\mathbf{e}^T\mathbf{P}\dot{\mathbf{e}} \\ &= -\frac{1}{2}\mathbf{e}^T(\mathbf{A}^T\mathbf{P} + \mathbf{P}\mathbf{A})\mathbf{e} + \mathbf{e}^T\mathbf{P}[-\mathbf{d}] + \mathbf{e}^T\mathbf{P}\mathbf{u}_s \\ &= -\frac{1}{2}\mathbf{e}^T\mathbf{Q}\mathbf{e} + \mathbf{e}^T\mathbf{P}[-\mathbf{d}] + \mathbf{e}^T\mathbf{P}\mathbf{u}_s \\ &\leqslant -\frac{1}{2}\mathbf{e}^T\mathbf{Q}\mathbf{e} + |\mathbf{e}^T\mathbf{P}| \cdot |\mathbf{d}| + \mathbf{e}^T\mathbf{P}\mathbf{u}_s \\ &\leqslant -\frac{1}{2}\mathbf{e}^T\mathbf{Q}\mathbf{e} + |\mathbf{e}^T\mathbf{P}| \cdot d_m + \mathbf{e}^T\mathbf{P}\mathbf{u}_s \end{aligned} \tag{III}$$

Substituting Eq. (23) in (III):

$$\begin{aligned} \dot{V} &\leqslant -\tfrac{1}{2}\mathbf{e}^T\mathbf{Q}\mathbf{e} + |\mathbf{e}^T\mathbf{P}| \cdot d_m + \mathbf{e}^T\mathbf{P}\left[\tfrac{|\mathbf{e}^T\mathbf{P}|}{(\mathbf{e}^T\mathbf{P})} \cdot (-I^*) \cdot d_m\right] \\ &\leqslant -\tfrac{1}{2}\mathbf{e}^T\mathbf{Q}\mathbf{e} + |\mathbf{e}^T\mathbf{P}| \cdot d_m \cdot [1 - I^*] \end{aligned} \tag{IV}$$

Since $I^* \geqslant 1$ right side terms of the above equation are negative and therefore the stability condition of the Lyapunov theory is satisfied. Note that by using control Eqs. (20) and (23), it can be concluded that $e \in L\infty$. Also by using the Barbalat's Lemma theory it can be realized that tracking error of the system is asymptotically stable

$(\lim_{t\to\infty} \mathbf{e} = 0)$.

References

[1] Song YH, Johns AT. Flexible AC transmission systems (FACTS). London: Institution of Electrical Engineers; 1999.
[2] Gyugyi L. A unified power flow control concept for flexible AC transmission systems. IEEE Proc – C 1992;139(4):323–31.
[3] Papic I, Zunko P, Povh D, Weinhold M. Basic control of unified power flow controller. IEEE Trans Power Syst 1997;12(4):1734–9.
[4] Yu Q, Rund SD, Norum LE, Undeland TM. Dynamic control of a unified power flow controller. IEEE Proc PESC 1996:508–14.
[5] Fujita H, Watanabe Y, Akagi H. Control and analysis of a unified power flow controller. IEEE Trans Power Electron 1999;14(6):1021–7.
[6] Makombe T, Jenkins N. Investigation of a unified power flow controller. IEEE Proc Gener Transm Distrib 1999;146(4):400–8.
[7] Tümay M, Vuralb AM, Loc KL. The effect of unified power flow controller location in power systems. Int J Electr Power Energy Syst 2004;26:561–9.
[8] Yam CM, Haque MH. A SVD based controller of UPFC for power flow control. Electr Power Syst Res 2004;70:76–84.
[9] Liu JY, Song YH, Mehta PA. Strategies for handling UPFC constraints in steady-state power flow and voltage control. IEEE Trans Power Syst 2000;15(2):566–71.
[10] Al-Mawsawi SA. Comparing and evaluating the voltage regulation of a UPFC and STATCOM. Int J Electr Power Energy Syst 2003;25:735–40.

[11] Chen H, Wang Y, Zhou R. Transient stability enhancement via coordinated excitation and UPFC control. Int J Electr Power Energy Syst 2002;24:19–29.
[12] Gholipour E, Saadate S. Improving of transient stability of power systems using UPFC. IEEE Trans Power Delivery 2005;20(2):1677–82.
[13] Leung JSK, Hill DJ, Ni Y. Global power system control using generator excitation, PSS, FACTS devices and capacitor switching. Int J Electr Power Energy Syst 2005;27:448–64.
[14] Kazemi A, Sohrforouzani MV. Power system damping using fuzzy controlled facts devices. Int J Electr Power Energy Syst 2007;28:349–57.
[15] Al-Awami AT, Abdel-Magid YL, Abido MA. A particle-swarm-based approach of power system stability enhancement with unified power flow controller. Int J Electr Power Energy Syst 2007;29:251–9.
[16] Guo J, Crow ML, Sarangapani J. An improved UPFC control for oscillation damping. IEEE Trans Power Syst 2009;14(1):288–96.
[17] Zou ZY, Jiang QY, Cao YJ, Wang HF. Application of the normal forms to analyze the interactions among the multi-control channels of UPFC. Int J Electr Power Energy Syst 2005;27:584–93.
[18] Ma TT. P-Q decoupled control schemes using fuzzy neural networks for the unified power flow controller. Int J Electr Power Energy Syst 2007;29:748–58.
[19] Schauder C, Mehta H. Vector analysis and control of advanced static var compensators. IEE Proc – C 1993;140(4):299–306.
[20] El-Hawwary MI, Elshafei AL, Emara HM, Fattah HAA. Output feedback control of a class of nonlinear systems using direct adaptive fuzzy controller. IEEE Proc Control Theory Appl 2004;151(5):615–25.
[21] Yu W, Moreno MA, Li X. Observer-based neuro identifier. IEEE Proc Control Theory Appl 2000;147(2):145–52.